INTERNATIONAL JOURNAL OF MULTIDISCIPLINARY RESEARCH AND ANALYSIS

ISSN(print): 2643-9840, ISSN(online): 2643-9875

Volume 07 Issue 12 December 2024

DOI: 10.47191/ijmra/v7-i12-25, Impact Factor: 8.22

Page No. 5561-5573

# Crack Propagation and Fatigue Life Analysis of Wind Turbine Blades

**Sam Prajwal Raj M**

PG Student, Aerospace and Automobile engineering M. S. Ramaiah University of applied sciences Bengaluru -560 054, India

**ABSTRACT:** This dissertation investigates the fatigue and fracture behaviour of wind turbine blades exposed to varying wind speeds and load intensities, aiming to enhance their durability and operational lifespan in sustainable energy systems. The increasing reliance on wind energy underscores the need for durable blades that can withstand cyclic loads and extreme environmental conditions, as fatigue and fracture failures significantly impact maintenance costs and reliability. This research specifically examines fatigue life and fracture initiation at wind speeds of 15 m/s and 60 m/s, analysing the effects of increased load intensities (30 MPa and 62 MPa).

Finite Element Analysis (FEA) through ANSYS is employed to model fatigue and fracture dynamics, incorporating fatigue life prediction using S-N curves, stress analysis with von Mises stress, and crack propagation simulation via fracture mechanics principles, such as Paris' Law. Results reveal a notable reduction in fatigue life with increased loads, evidenced by a drop from 9e09 to 7.9e08 cycles at 15 m/s, with comparable fatigue cycle reductions at 60 m/s. Fracture analysis identifies critical crack initiation points in high-stress areas, and simulations indicate the progressive nature of crack propagation under cyclic loads.

These findings underscore the importance of integrating fatigue and fracture assessments in the design and maintenance strategies of wind turbine blades to enhance resilience and support the sustainable advancement of wind energy systems.

**KEYWORDS:** Fracture, Fatigue, Composite materials, Computational analysis, Renewable energy, Wind turbine blades, Fluent Analysis, Structural analysis

## I. INTRODUCTION

Wind turbine blades, as essential components of wind energy systems, are subjected to cyclic loading and various environmental stressors throughout their operational lifetime. These persistent conditions make turbine blades highly susceptible to fatigue and fracture failures, directly impacting the efficiency, durability, and safety of wind turbines. This dissertation aims to examine these critical issues by performing an in-depth fatigue and fracture analysis under varying wind speeds and load conditions. A central focus is placed on understanding how increased loading, especially under high-speed conditions, influences fatigue life and the initiation of fractures in turbine blades. The study integrates Finite Element Analysis (FEA) with experimental methodologies in fatigue and fracture mechanics to predict the behaviour of turbine blade materials. By exploring the relationships among cyclic stresses, material deformation, and crack propagation, this research seeks to provide valuable insights that can guide the optimization of structural design and material selection for wind turbine blades. Bridging the gap between aerodynamic efficiency and structural resilience, the work aims to enhance understanding of failure mechanisms and to support strategies for mitigating blade failure. The importance of this research lies in its potential to reduce costly maintenance and operational downtime resulting from premature fatigue and fracture failures. The findings are expected to extend the operational life of wind turbine blades, thereby increasing the overall reliability of wind energy systems. By employing fatigue and fracture theories, such as Paris' Law and S-N curve analysis, this study establishes a framework for predicting failure and strengthening blade design to endure harsh operational conditions.

## II.LITERATURE REVIEW

Crack propagation and fatigue life analysis are crucial in understanding the structural integrity and durability of wind turbine blades, which experience continuous loading cycles due to fluctuating wind speeds. Early research emphasizes the cyclic loading experienced by blades, especially in offshore environments, and its contribution to material fatigue. Models like Paris' Law and Miner's Rule are commonly employed for predicting crack initiation and growth. Crack propagation studies typically focus on:

Aerodynamic loading and stress distributions across the blade length. Material behavior under cyclic fatigue, particularly in composite materials like Glass Fiber Reinforced Plastic (GFRP) and Carbon Fiber Reinforced Plastic (CFRP). The impact of environmental factors, such as moisture absorption, UV exposure, and temperature fluctuations, which further accelerate crack growth.

**Efstathios E. Theotokoglou, Georgios Xenakis "GE 1.5 XLE Wind Turbine Blade Analysis with Computational Methods for Various Composite Materials** [1] Summary: Composite Material Analysis: The paper explores the structural behavior of wind turbine blades made from various composite materials, such as E-Glass, Kevlar, Solvay APC-2/AS4 Carbon Fiber, S-Glass, and S-2 Glass, using finite element analysis. ANSYS Fluent and structural analysis tools are employed to determine stress distributions, displacements, and aerodynamic properties of the GE 1.5 XLE wind turbine blade.

**Silvain A. Michel, Rolf Kieselbach, Hans Jörg Martens "Fatigue Strength of Carbon Fiber Composites up to the Gigacycle Regime"**[2] Summary: Fatigue Behavior in Gigacycle Regime: The paper investigates the fatigue performance of carbon fiber composites (AS4/APC-2) in the gigacycle regime, beyond $10^6$ cycles. It identifies a significant decrease in fatigue strength as the number of cycles increases, with no clear fatigue limit, highlighting the gradual degradation of material properties under prolonged cyclic loading.

**Sanaa El Mouhsine , Karim Oukassou, Mohammed Marouan Ichenial, Bousselham Kharbouch, Abderrahmane Hajraoui " Aerodynamics and structural analysis of wind turbine blade"**[3]Summary: The finite element model effectively combines aerodynamics and static structural analyses to understand the behavior of Horizontal-Axis Wind Turbine (HAWT) blades under various conditions. Optimal blade design, defined by aerodynamic calculations and efficient airfoil shapes, is crucial for maximizing aerodynamic performance despite potential aeroelastic instabilities. Accurate modeling and simulation of both fluid and structural meshes are essential for detailed structural and aeroelastic analysis, contributing to enhanced turbine performance and reduced power loss.

**S.Karthik1 K.Muralidharan , D.Vazudevan " DESIGN AND STRUCTURAL ANALYSIS OF WIND TURBINE BLADE USING FINITE ELEMENT SOFTWARE "**[4]Summary: The study effectively demonstrates the use of Finite Element Analysis (FEA) software to evaluate deflection and stress values for steel and Carbon Fiber Reinforced Plastic (CFRP) materials, validating the procedure with both FEA and mathematical calculations. Composite materials like CFRP are preferred for turbine blade design due to their lower weight, cost-effectiveness, and ease of transportation, which contribute to improved power generation efficiency. The analysis indicates that while steel blades experience significant deflection under load, CFRP blades offer better performance with reduced deflection and stress, making them a more suitable material choice for turbine blades.

**C. Amer, M. Sahin " Structural Analysis of a Composite Wind Turbine Blade "**[5] Summary: The optimized 5-meter-long horizontal axis wind turbine rotor blade was successfully modeled using airfoil geometries, transferred to a finite element modeling environment, and assigned appropriate material properties for detailed dynamic and static behavior analysis. Various analyses, including mesh independency checks and evaluations of boundary conditions and layer orientation configurations, revealed that the blade's stiffness could be improved by orienting all layers in the 0-degree direction. The study found significant coupling in the normal modes, necessitating further investigation through experimental modal testing, which is currently in progress.

**Balakumaran Natarajan, Jaehwan Lee , Jaehoon Lim , and SangJoon Shin" Structural Analysis of Composite Wind Turbine Blade using Advanced Beam Model Approach"**[6]Summary: The structural analysis of a 10-kW wind turbine blade, designed with a single-cell cross-section using CFRP and aluminum reinforcement at the root, demonstrated the effectiveness of an advanced beam modeling approach. This approach, integrating two-dimensional cross-sectional and one-dimensional beam analyses, achieved geometric exactness with reduced computational effort and maintained consistency with three-dimensional elasticity theory.

**Vedulla Manoj Kumar, B Nageswara Rao, Sk. Farooq "Modeling and analysis of wind turbine blade with advanced materials by simulation"**[7] Summary: Transition from epoxy glass to epoxy carbon in wind turbine blades enhances performance, reducing total deformation and improving stress resistance. ANSYS Workbench software validates superior structural integrity of epoxy carbon through static and dynamic analyses. Results show epoxy carbon outperforms epoxy glass in minimizing deformation and stress, crucial for optimizing wind turbine efficiency and reliability.

**Lin Wang, Robin Quant, Athanasios Kolios "Fluid structure interaction modelling of horizontal-axis wind turbine blades based on CFD and FEA"**[8]Summary: The paper presents the development of a fluid-structure interaction (FSI) model for large wind turbine blades, specifically the Wind PACT 1.5 MW horizontal-axis wind turbine blade. The model combines computational fluid dynamics (CFD) for aerodynamic load calculations and finite element analysis (FEA) for structural response assessment. A one-way coupling strategy is used, where aerodynamic loads calculated from the CFD model are mapped to the FEA model as load boundary conditions. This approach is chosen for its computational efficiency. The developed FSI model is validated through benchmark tests and applied to the Wind PACT 1.5 MW wind turbine blade. The results show that the maximum stresses and deflections are within material and structural limits under various operational conditions.

**Wang, W., Xue, Y., He, C. and Zhao, Y " Review of the Typical Damage and Damage-Detection Methods of Large Wind Turbine Blades"**[9] Summary: The paper comprehensively summarizes the common types of faults and defects in wind turbine blades, such as trailing edge cracking, lightning strikes, leading edge corrosion, icing, and delamination. It delves into the primary generation mechanisms of these defects, emphasizing the impact of harsh external environmental.

**III.METHODOLOGY OF PROPOSED SURVEY**

The methodology for this research is designed to systematically address each objective and provide a comprehensive understanding of fatigue and fracture behavior in wind turbine blades. Initially, surface crack-prone zones are identified through high-stress concentration analysis by setting up a structural analysis framework. This involves both aerodynamic analyses using ANSYS Fluent and static structural analysis within ANSYS, utilizing specific material properties, aerodynamic profiles, and blade geometry data. Once these high-stress areas are identified, the next step involves performing a detailed fatigue analysis to predict the blade's lifespan under varying loads. Using established theories such as Miner's Rule and S-N Curves (Wohler Curves), the fatigue analysis provides insight into the blade's endurance limits based on fatigue data specific to the materials used. In the final phase, modeling of cracks in identified failure zones is undertaken using techniques like cohesive zone modeling, which facilitates accurate simulation of crack growth under complex loading conditions. This phase involves the application of fatigue loads, particularly centrifugal forces, to represent real-world operational stresses. The crack propagation is then simulated under axial-torsion-shear coupling loads to observe how cracks advance in both metal and composite blade materials, with a focus on key factors such as critical crack length and propagation direction. This integrated methodology ensures that each phase builds upon the previous, enabling a detailed and realistic analysis of fatigue and fracture mechanisms in wind turbine blades.

**IV. ANALYSIS OF GE 1.5XLE WIND TURBINE BLADES**

A wind turbine blade's aerodynamic optimum model refers to the blade design with the smallest achievable thickness. However, safety is an essential component of its design, which considers unknown features of its loads, material deterioration, and potential flap failure. However, in many situations, the safety factors are very high, resulting in superstructures. To more accurately identify safety considerations, extensive information on the impacts of different loading situations (high winds, humidity, temperature fluctuations) and parameters on the structures of the composite materials of the blades in terms of durability and life expectancy is employed, [1]. Computational models or theoretical research on the behavior of blades under various loading circumstances can provide the essential knowledge. A variety of analytical and numerical methodologies are necessary to address failures. Analytical approaches employed include models based on residual shear stresses, generalised fibre bundle models, failure processes, and mechanism-based models. In residual shear stress models, force equilibrium assumes that only shear and fibre loads are communicated. In general, fibre bundle models use statistical fibre strength models and a variety of stress circumstances. According to earlier research, the goal is to model the failure of composite wind turbines [1]. The finite element approach is most commonly used to solve issues, in which integrals and differential equations representing material deformations and microstructures are derived using body discretisation and equation approximation. Complex models of wind turbine blades, even with damaged materials, are a good candidate for considerable investigation using the methods described above [1]. In this work, we analyse the GE 1.5XLE wind turbine blades using the finite element approach, starting with the ANSYS Fluent tool [1]. The approach used is Computational Fluid Dynamics (CFD). The answer came from the ANSYS 19.2 Workbench software suite. Fluid Fluent and Static Structural [1] were employed with Computer Aided Engineering (CAE) design, modelling, analysis, and processing results in mind. The model was created and solved in two sections. First, the Fluent was solved, followed by the Structural. The first model was created to solve aerodynamic loads on the flap, and the second used the estimated loads to determine the stresses on the flap and its displacements. The second model was tested using five materials. These include E-Glass Fibre, Generic, Solvay APC-2/AS4 PEEK Plus Carbon Fibre Reinforced Unidirectional Tape, DuPont™ Kevlar® 49 Aramid Fibre, S-Glass Fibre, Generic, and S-2 Glass Fibre, Generic. We consider all five materials to be macroscopic isotropic since they have identical stress levels in random directions. Table 1 [4] shows the material qualities. The research was motivated by a previous study conducted by Sebastian Lachance-Barrett and Robert Zhang, Professor of Wind Energy at Cornell University in New York [4]. General Electric created the GE 1.5XLE wind turbine type. It produces 1500 kW and can run in winds as low as 3.5 m/s and as high as 20 m/s. It is wind resistant up to 52.5 m/s. Its rotor is 82.5 meters in diameter and spans an area of 5346 square meters. It is made of a composite material that includes glass fibres

### 4.1 Fluent Analysis

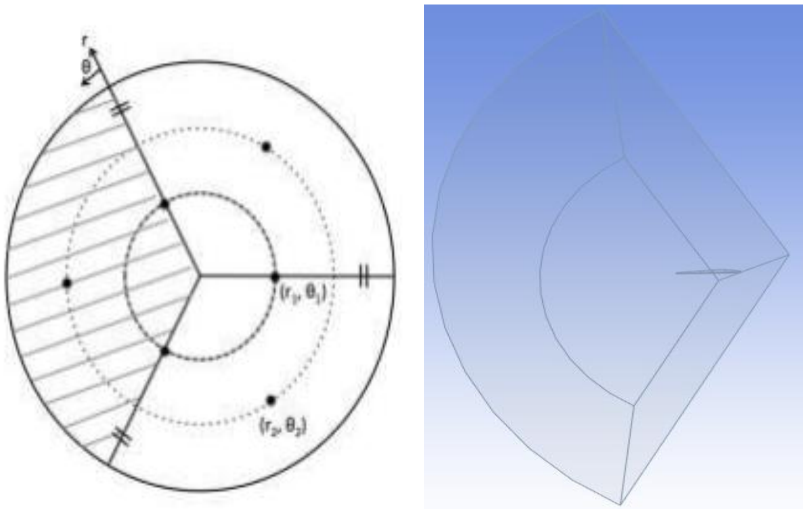


**Figure 1 considering 1/3 of the problem**

Boundary conditions in the fluid region are:

1. Inlet: Velocity of 15 m/s with turbulent intensity of 5% and turbulent viscosity ratio of 10

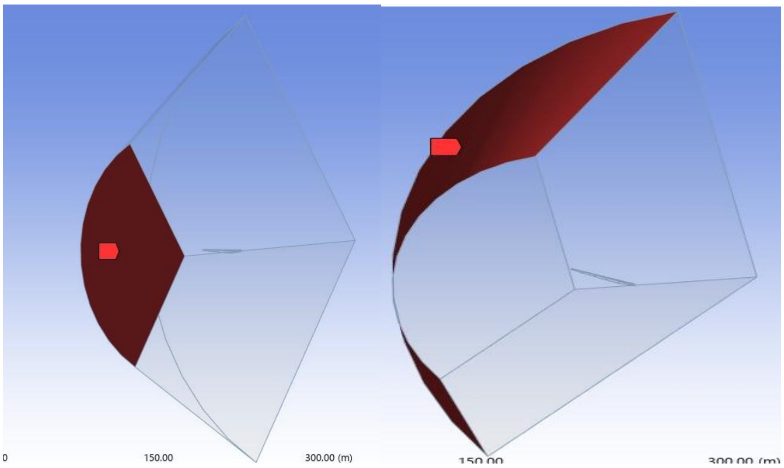


**Figure 2 Inlet Boundary Condition**

2. Outlet: Taking a Pressure of 1atm.

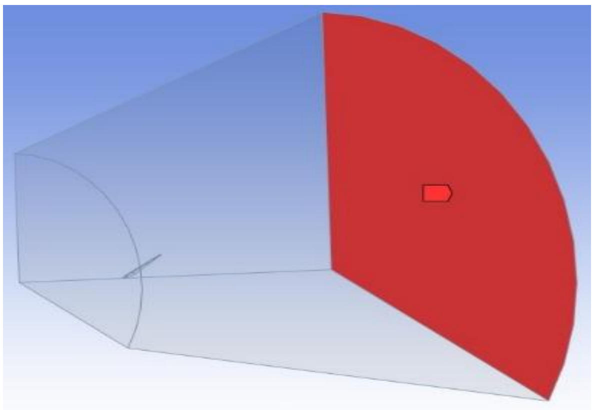

**Figure 3 Outlet Boundary Condition**

3. Blade: Taken to be as a No Slip-Wall

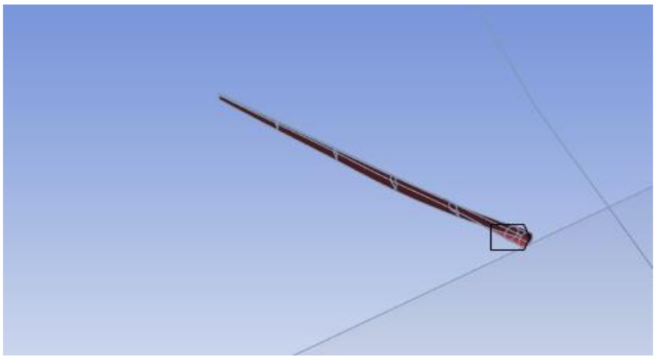

**Figure 4 Blade as wall Boundary Condition**

4. Quadrilateral Boundaries: Periodic.

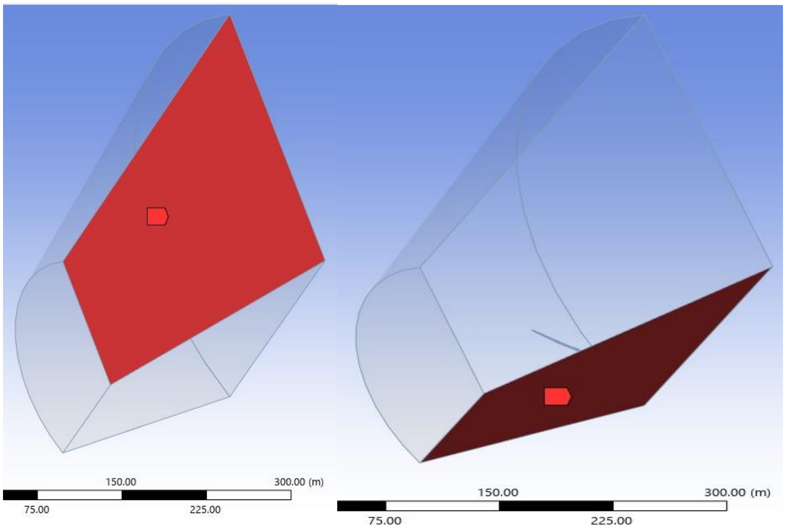


**Figure 5 Periodic Boundary Condition**

According to Figure 6, the finite element mesh has around 400,000 triangular and tetrahedral elements. The generated matrices are thought to be significantly sparing as matrices despite their high volume. A solvent based on pressure is used by Ansys [1]. The wind turbine's geometry was used from the Cornell University website [1]. In Figure 1, we first see the fluid (air) that surrounds one wind turbine blade and takes up the bulk volume. The fluid domain is conical in shape, having a radius of 120 meters in front of the blade and 240 meters behind it. The fluid flows from the front to the rear of the blade throughout its 270-meter length.

**Table I Properties of the materials**

| Name | Density (Kg/m3) | Young Modulus (GPa) | Poisson's Ratio | Shear Modulus (GPa) |
|---|---|---|---|---|
| E-Glass Fibre | 2.565 | 72.4 | 0.2 | 30 |
| Kevlar Aramid Fibre | 1.437 | 112 | 0.36 | 7 |
| Solvay APC2/AS4 Carbon Fibre | 1.319 | 138 | 0.3 | 5.7 |
| S-Glass Fibre | 2.482 | 86.3 | 0.22 | 35 |
| S-2 Glass Fibre | 2.457 | 86.9 | 0.23 | 35 |

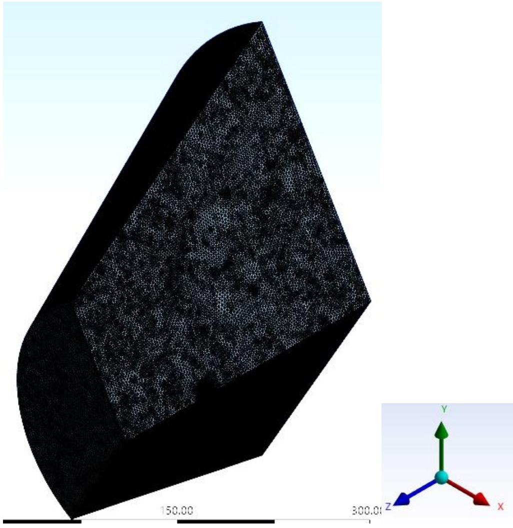


**Figure 6 Ansys Fluent Mesh**

The inlet sections and the inlet top on the Z-axis have been taken into consideration as boundary conditions for speed entrance (Figure 2). On the Z-axis, a negative speed of 15 m/s entered. The degree of viscosity was 10 and the vortex intensity was 5%. A portion with an outlet pressure equal to atmospheric pressure is achieved as an outlet. Furthermore, because we have picked one-third of the geometry, we have regarded periods 1 and 2 as interface points rather than walls. Lastly, the fluid portion contained the interior kind. A speed of 88 m/s is anticipated at the blade ends based on the preliminary pre-analysis calculations, and our fluent exported a speed of 98 m/s, which is an acceptable result for our model.

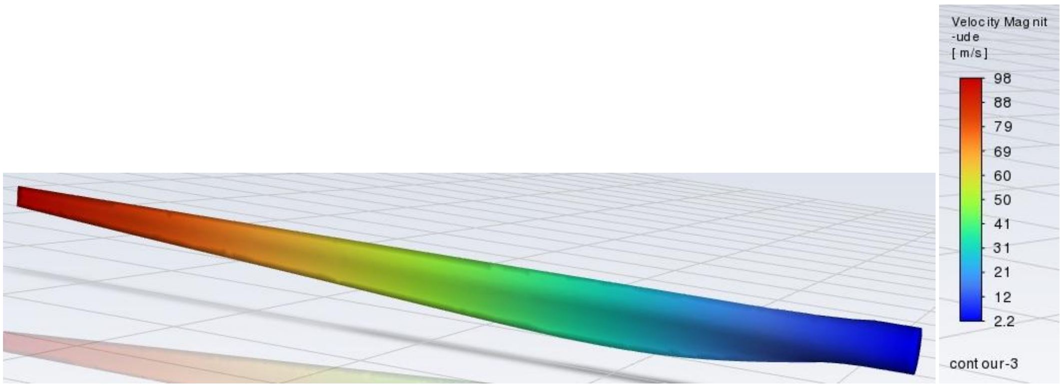


**Figure 7 Velocity Contour from Fluent Setup is 98m/s**

The wind speed profile from both the entrance and the outflow is displayed in Figure 7. As anticipated, the initial speed at the entry is 15 m/s. A decrease in speed may be seen behind the blade, indicating proper behaviour. Lastly, a few orange lines around the blades' rotation show a higher speed, which likewise denotes the right answer

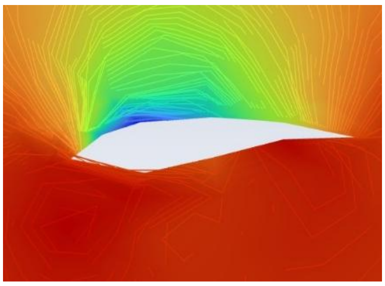

**Figure 8 Pressure Contour cut section around The Airfoil**

Next, we examine the wind turbine's pressure profile in Figure 8. The front is under more strain than the back, which was to be expected. The convergence of the solution from the finite element findings in relation to the number of iterations is another significant issue. Figure 9 shows a solution convergence of 10-6 residuals and good solution behavior.

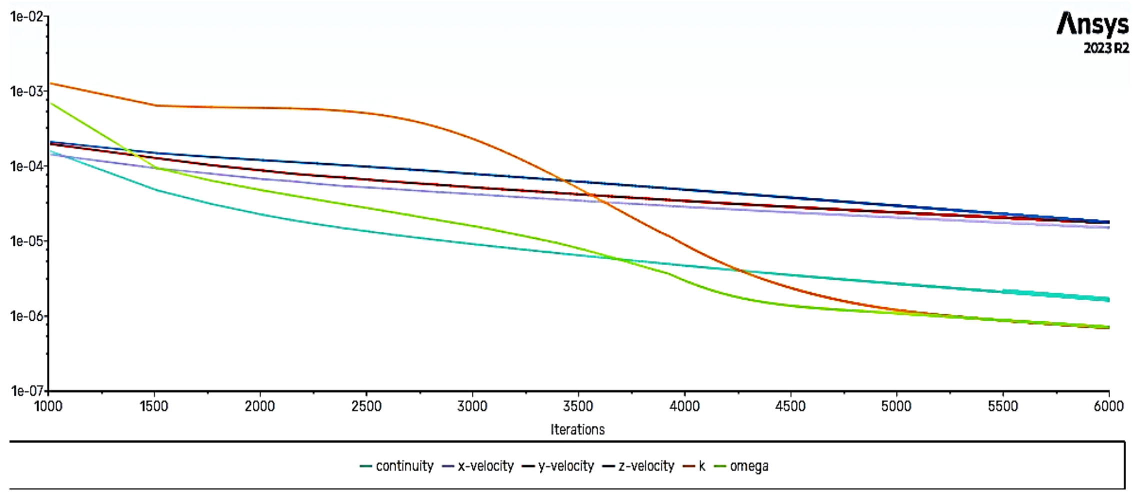


**Figure 9 Residual Plot from Ansys Fluent**

**4.2 Structural Analysis**

The structural analysis includes the static study of the blade. The pressure on the blade is calculated using the results from the fluent study and then the stresses and displacements fields are calculated. The blade consists of an outer surface and an inner beam.

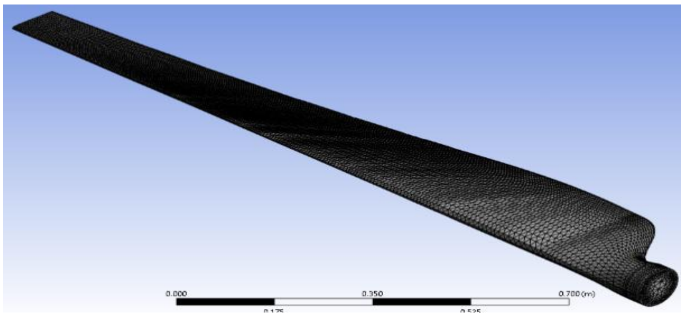

**Figure 10 Ansys Mechanical Mesh**

**Figure 11 Ansys Boundary Condition Displacement Constraint**

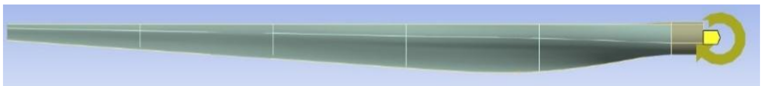

**Figure 12 Ansys Structural Rotational Velocity**

The mathematical model for static analysis is based on Shell theory. This is a development of Euler-Bernoulli's beam theory. The blade's finite element mesh was designed with an element size of 20 cm. The mesh has several sorts of elements (triangular, tetrahedral, etc.). They took roughly 5,403 finite elements, which is almost 90 times fewer than the Fluent analysis. Initially, the overall displacements are determined. Figure 14 shows that the blade shifts as predicted. The largest displacements occur near the tip of the blade, and as we approach the root of the blade, displacements decrease in all of the analyzed situations. In Table 2, the maximum displacements according to the different materials are given. It is observed that Solvay APC-2/AS4 Carbon has the minimum displacement.

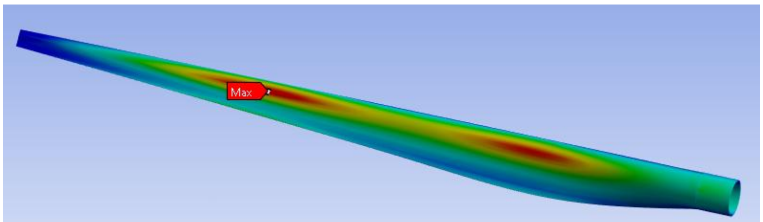


**Figure 13 Stress Plot under 60m/s Inlet Velocity [Solvay APC2/AS4 Carbon Fiber]**

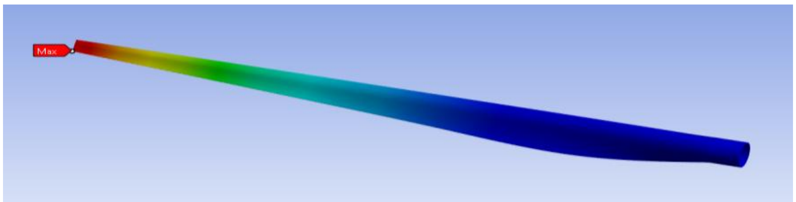


**Figure 14 Total Structural Deformation under 60m/s Inlet Velocity [Solvay APC2/AS4 Carbon Fiber]**

**Table II Material Deflection for 15 m/s Inlet Velocity**

| Material Deflection | Result from Paper [1] | Results from Simulation |
|---|---|---|
| E-glass | 0.698 m | 0.73 m |
| Kevlar | 0.488 m | 0.52 m |
| Carbon Fiber | 0.414 m | 0.43 m |
| S-Glass | 0.589 m | 0.644 m |
| S-Glass 2 | 0.6 m | 0.641 m |

**Table III Material Stresses For 15 m/s Inlet Velocity**

| Material Stresses | Result from Paper [1] | Results from Simulation |
|---|---|---|
| E-glass | 30.66 Mpa | 32.549 Mpa |
| Kevlar | 32.55 Mpa | 35.357 Mpa |
| Carbon Fiber | 34.084 Mpa | 36.147 Mpa |
| S-Glass | 31.776 Mpa | 33.897 Mpa |
| S-Glass 2 | 31.655 Mpa | 33.941 Mpa |

**Table IV Material Deflection for 60 m/s Inlet Velocity**

| Material Deflection | Result from Paper [1] | Results from Simulation |
|---|---|---|
| E-glass | 1.567 m | 1.456 m |
| Kevlar | 1.115 m | 1.057 m |
| Carbon Fiber | 0.945 m | 0.891 m |
| S-Glass | 1.322 m | 1.268 m |
| S-Glass 2 | 1.348 m | 1.262 m |

**Table V Material Stresses For 60 m/s Inlet Velocity**

| Material Stresses | Result from Paper [1] | Results from Simulation |
|---|---|---|
| E-glass | 63.22 Mpa | 62.77 Mpa |
| Kevlar | 65.47 Mpa | 64.815 Mpa |
| Carbon Fiber | 69.26 Mpa | 67.99 Mpa |
| S-Glass | 64.45 Mpa | 63.96 Mpa |
| S-Glass 2 | 64.24 Mpa | 63.92 Mpa |

### 4.3 Fatigue Analysis

The consistency between the von Mises stresses from the paper[1] and simulation results provides a strong basis for analyzing fatigue life and potential crack initiation points. Areas where the stress exceeds material strength limits may exhibit crack initiation, especially in high-stress regions. This emphasizes the need for local fracture mechanics analysis, as mentioned earlier.


**Figure 15 Fatigue Life at 15 m/s and 60m/s Inlet Velocity**

## Crack Propagation and Fatigue Life Analysis of Wind Turbine Blades

To assess the blade's performance under more extreme loading conditions, the load was scaled by 20 times. This approach simulates how the materials would behave under excessive wind loads or unexpected extreme operating conditions. When the load was increased, the fatigue life reduced to 7.94e08 cycles, a decrease in the material's life expectancy. However, this reduction is comparatively moderate, suggesting that the materials retain substantial structural integrity even under amplified load conditions. The materials are resilient, but prolonged exposure to such loads could eventually lead to fatigue failure. The drastic drop from 9.95e08 cycles to 494.44 cycles when the load is scaled by 20 times illustrates that while the material is well suited for normal operational conditions, excessive loads pose a significant threat. The materials are not designed to withstand such extreme loads for extended periods, and failure would occur rapidly if these conditions were to persist.

This contrast highlights that fatigue failure is highly dependent on the magnitude of the load, and increasing the load significantly reduces the material's ability to resist cyclic stress.

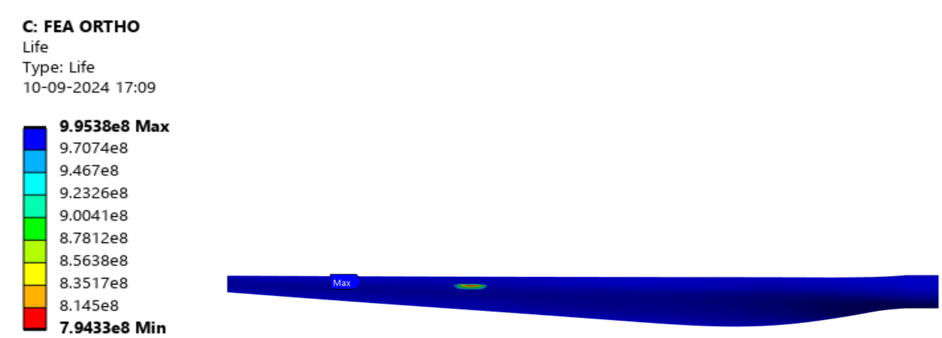


**Figure 16 Fatigue Life at 15 m/s Inlet Velocity for Scaled loads**

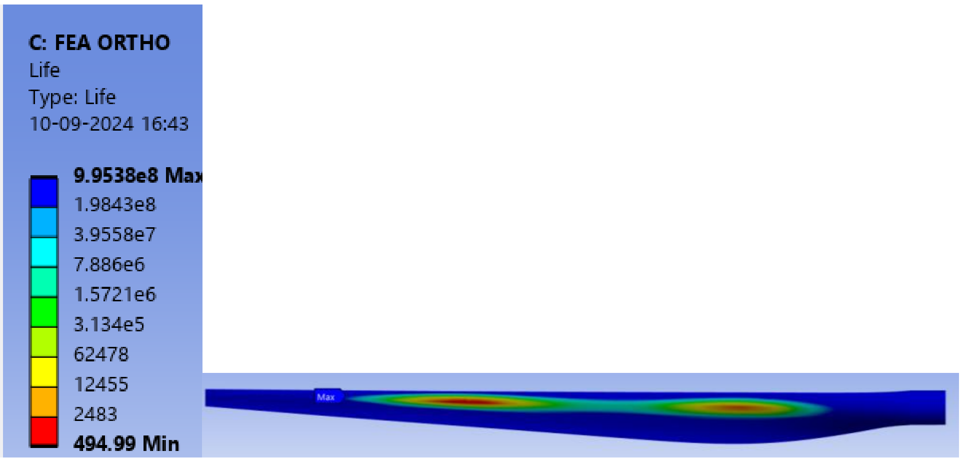


**Figure 17 Fatigue Life at 60 m/s Inlet Velocity for Scaled loads**

### 4.4 Fracture Analysis

In the context of local analysis of the wind turbine blade, we transformed a high-stress concentration region into a flat plate to simplify and focus the analysis on stress intensity factors and total deformation. This method isolates the crack propagation and its interaction with the stress field, providing more precise insights into the structural integrity of the blade at various crack lengths and wind velocities.

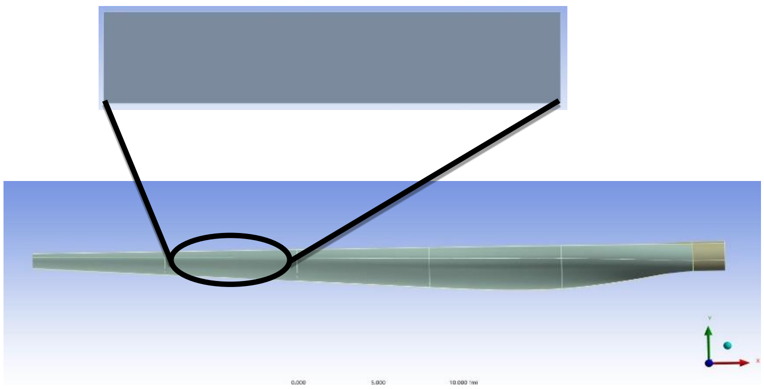

**Figure 18 Part of blade considered as a Flat Plate for Local Analysis**

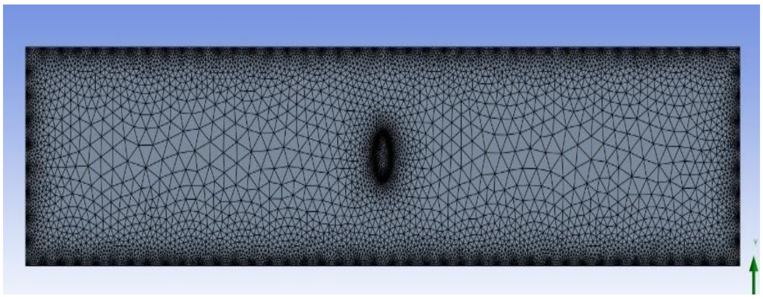

**Figure 19 Tetrahedron Mesh of Elliptical Crack For the local analysis**

The wind turbine blade section, a tetrahedral mesh was employed to ensure that complex geometries, such as the crack propagation and stress concentration regions, were captured with high accuracy. The choice of a tetrahedral mesh allowed for detailed representation of the curved and irregular surfaces of the plate, providing an accurate approximation of the stress distribution. Mesh Type: Tetrahedral mesh. Total Node Count: 230,456 nodes. The tetrahedral mesh, consisting of 230,456 nodes, was chosen to balance the need for computational efficiency with the accuracy of the results. A denser mesh was applied in regions close to the crack tip and areas of high stress intensity to ensure that small-scale stress variations were captured effectively. This higher node density is especially crucial for calculating stress intensity factors (K1, K2, K3) with high precision, as it minimizes interpolation errors that could occur in regions with complex stress gradients.

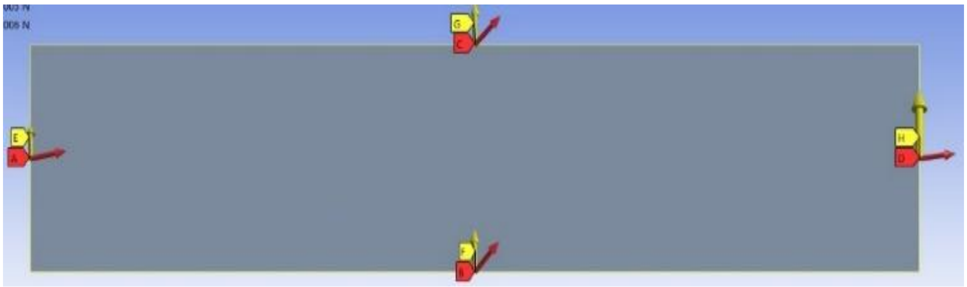

**Figure 20 Force and Displacement constraint on Blade**

Boundary Condition for Local Analysis: The constraints define how much the edges of the flat plate can move under specific boundary conditions. Each side of the flat plate has specific displacement components in the X, Y, and Z directions. The values need is applied as boundary conditions to the local flat plate model in the analysis. Displacement and Applied Force boundary conditions need to be applied at the respective side of the flat plate model.

**Table VI Displacement constraint For Inlet 15m/s**

| Side number | X in m | Y in m | Z in m |
|---|---|---|---|
| E | 2.1792E-04 | 5.7716E-02 | -4.5566e-02 |
| F | -4.1792E-04 | 5.7716E-02 | -4.5566E-02 |
| G | 2.1792E-04 | 5.7685E-02 | -6.9255E-03 |
| H | -5.66196E-05 | 1.1932E-02 | -62338E-03 |

**Table VII Displacement constraint For Inlet 60m/s**

| Side number | X in m | Y in m | Z in m |
|---|---|---|---|
| E | 4.17E-03 | 0.12652 | -9.746E-02 |
| F | -1.2298E-03 | 0.12651 | -4.221E-02 |
| G | 4.179E-03 | 0.12645 | -4.23E-02 |
| H | 1.742E-04 | 6.675E-02 | -4.22E-02 |

**Table VIII Applied Force for Inlet 15m/s**

| Side number | X in N | Y in N | Z in N |
|---|---|---|---|
| A | 6.7668E05 | 1.18106E05 | 79022 |
| B | 4.6719E05 | 1.8106E05 | 79022 |

| | | | |
|---|---|---|---|
| C | 5.4415E05 | 5.288E05 | 1.86E05 |
| D | 1.1596E06 | 1.3467E05 | 1.1537E05 |

**Table IX Applied Force for Inlet 60m/s**

| Side number | X in N | Y in N | Z in N |
|---|---|---|---|
| A | 3.9593E06 | 1.65E06 | 62815 |
| B | -5715.6 | 1.0376E06 | 3.5723E05 |
| C | 6.290E05 | 1.013E06 | 3.1819E06 |
| D | 3.2725E06 | 7.9338E05 | 3.86E06 |

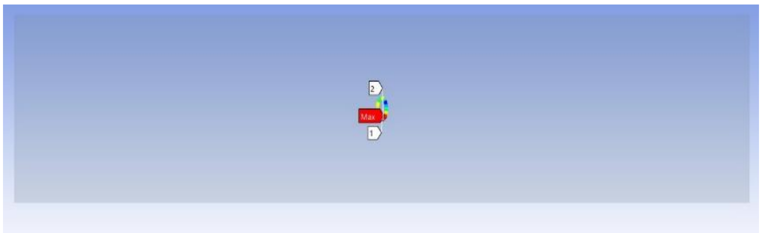

**Figure 21Stiffness Matrix on the Plate**

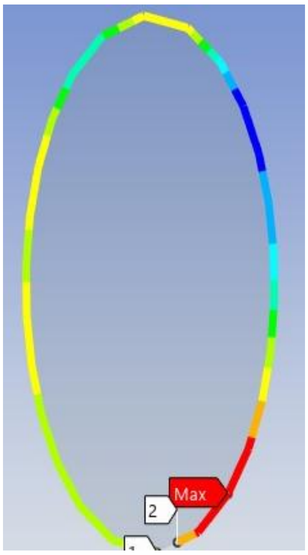


**Figure 22 Magnified view of Stiffness Matrix K1 of the Plate**

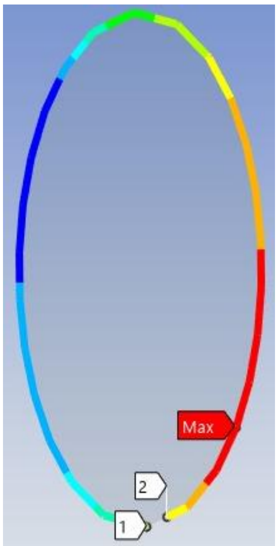


**Figure 23 Magnified view of Stiffness Matrix K2 of the Plate**

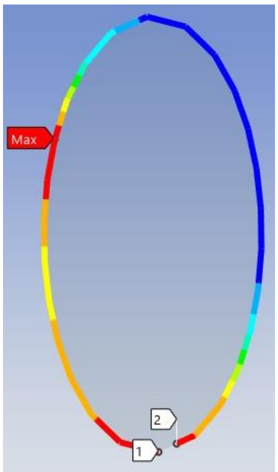


**Figure 24 Magnified view of Stiffness Matrix K3 of the Plate**

**Table X Stress Intensity Factors of various crack length for 15m/s Inlet Velocity**

| MAJOR AXIS(m) | MINOR AXIS(m) | Stiffness K1 MPa√m | Stiffness K2 MPa√m | Stiffness K3 MPa√m |
|---|---|---|---|---|
| 5e-02 | 2.5e-02 | 1.201 | 3.21 | 0.8609 |
| 2e-02 | 1e-02 | 1.0807 | 1.7869 | 0.41797 |
| 0.1 | 0.05 | 2.38 | 14.648 | 1.0621 |
| 0.2 | 0.1 | 0.07194 | 10.172 | 0.407 |
| 0.3 | 0.15 | 0.6577 | 6.62 | 0.473 |
| 0.4 | 0.2 | 0.365 | 17.99 | 0.250 |
| 0.1 | 0.04 | 7.75 | 18.85 | 0.092664 |
| 0.1 | 0.5 | 5.21 | 10.326 | 0.818 |
| 0.1 | 4E-02 | 0.3071 | 35.963 | 8.286 |
| 0.1001 | 4E-02 | 0.345 | 39.72 | 6.48 |
| 0.1002 | 4E-02 | 0.352 | 39.75 | 1.234 |
| 0.1085 | 4E-02 | 0.5106 | 46.355 | 8.18 |
| 0.107 | 4E-02 | 0.497 | 48.23 | 8.342 |
| 0.106 | 4E-02 | 0.469 | 48.46 | 12.639 |
| 0.10559 | 4E-02 | 0.483 | 49.55 | 6.804 |

**Table XI Stress Intensity Factors of various crack length for 60 m/s Inlet Velocity**

| MAJOR AXIS(m) | MINOR AXIS(m) | Stiffness K1 MPa√m | Stiffness K2 MPa√m | Stiffness K3 MPa√m |
|---|---|---|---|---|
| 5e-02 | 2.5e-02 | 5.107 | 8.3751 | 0.9141 |
| 2e-02 | 1e-02 | 11.375 | 3.60 | 4.46 |
| 0.5 | 0.25 | 0.08319 | 2.9167 | 0.739 |
| 0.1 | 5e-02 | 5.532 | 17.20 | 0.607 |
| 0.1 | 0.5 | 1.14 | 34.51 | 3.533 |
| 0.2 | 0.1 | 1.89 | 19.109 | 0.31548 |
| 0.4 | 0.1 | 1.6 | 35.41 | 1.06 |
| 0.5 | 0.1 | 0.681 | 44.52 | 2.065 |

At an inlet velocity of 15 m/s, the analysis reveals that crack propagation in the wind turbine blade is predominantly influenced by shear forces, as reflected in high Mode II (K2) values across various crack configurations. For instance, with a major axis of 0.1 m and a minor axis of 0.04 m, the high K2 (35.963 MPa√m) value indicates a significant shear-driven crack propagation, while the twisting component (K3) introduces complexity to the crack path. Tensile forces (K1) play a secondary role, suggesting that blade durability may be enhanced by focusing on shear resistance. This moderate aerodynamic loading scenario suggests the blade is highly susceptible to shear-induced cracking, underscoring the need for robust design considerations to handle mixed-mode stress impacts.

At a higher inlet velocity of 60 m/s, shear forces remain dominant in driving crack propagation, yet tensile stresses also become increasingly influential in some configurations. For example, with a smaller crack (major axis 0.02 m), K1 reaches 11.375 MPa√m, indicating a strong tensile opening effect that could accelerate crack propagation. Additionally, larger cracks (major axis 0.5 m) show continued shear dominance (K2 at 44.52 MPa√m), while K3 introduces minor twisting effects. The findings suggest that under high-velocity aerodynamic conditions, the blade faces a combination of tensile, shear, and twisting stresses, demanding advanced design features to counter these complex loading patterns and improve fracture resistance

## V. CONCLUSIONS

The fatigue life analysis and fracture mechanics study of the wind turbine blade under cyclic loading provided key insights into its deformation, stress distribution, and crack behavior. The structural analysis highlighted high-stress concentration regions, notably near the blade root and mid-span, where von Mises stresses indicated potential areas for fatigue failure. Fatigue life analysis showed a significant reduction in life cycles, especially under increased loads, with a drop from 9e09 to 7.9e08 cycles in critical regions. Stress intensity factor analysis revealed that shear stresses (K2, Mode II) are the primary drivers of crack propagation in these areas, suggesting a shear-dominant failure mode under bending and torsional forces. A focused study of the high-stress zones using a flat plate model further underscored the influence of Mode II stresses on crack initiation and growth, indicating that the blade's material may require enhanced shear resistance to withstand cyclic loading and improve fatigue life.

This study highlights critical areas for advancing wind turbine blade design, focusing on the dominant role of shear stresses (K2) in crack propagation within composite materials. Future research should consider advanced 3D crack propagation models like cohesive zone modeling and XFEM for a more realistic depiction of cracks in composite layers. Exploring materials optimized for shear resistance, such as hybrid composites, could reduce mode-II related fatigue. A full, non-linear analysis of entire blades would deepen understanding of real-world operational impacts, while experimental validation using scaled prototypes and digital image correlation could confirm findings. Integrating blade dynamics with overall turbine system dynamics through fluid-structure interaction and exploring geometry optimization can help mitigate stress concentrations, ultimately enhancing blade durability and reducing maintenance needs.

## REFERENCES

1) Theotokoglou, E. E., & Xenakis, G. (2023). GE 1.5 XLE Wind Turbine Blade Analysis with Computational Methods for Various Composite Materials. WSEAS Transactions on Applied and Theoretical Mechanics, 18, 56-63. doi:10.37394/232011.2023.18.6.
2) Michel, S. A., Kieselbach, R., & Martens, H. J. (2006). Fatigue Strength of Carbon Fibre Composites up to the Gigacycle Regime. International Journal of Fatigue, 28(3), 261-270. doi:10.1016/j.ijfatigue.2005.05.005.
3) Wu, W.H. and Young, W.B., 2012. Structural analysis and design of the composite wind turbine blade. Applied Composite Materials, 19, pp.247-257.
4) Karthik, S., Muralidharan, K. and Vasudevan, D., DESIGN AND STRUCTURAL ANALYSIS OF WIND TURBINE BLADE USING FINITE ELEMENT SOFTWARE.
5) Amer, C. and Sahin, M., 2014. Structural analysis of a composite wind turbine blade. International Journal of Aerospace and Mechanical Engineering, 8(7), pp.1264-1270.
6) Natarajan, B., Lee, J., Lim, J. and Shin, S., 2012. Structural analysis of composite wind turbine blade using advanced beam model approach. International Journal of Precision Engineering and Manufacturing, 13, pp.2245-2250.
7) El Mouhsine, S., Oukassou, K., Ichenial, M.M., Kharbouch, B. and Hajraoui, A., 2018. Aerodynamics and structural analysis of wind turbine blade. Procedia Manufacturing, 22, pp.747-756.
8) Kumar, V.M., Rao, B.N. and Farooq, S., 2016. Modelling and analysis of wind turbine blade with advanced materials by simulation. International Journal of Applied Engineering Research, 11(6), pp.4491-4499.
9) Wang, L., Quant, R. and Kolios, A., 2016. Fluid structure interaction modelling of horizontal-axis wind turbine blades based on CFD and FEA. Journal of Wind Engineering and Industrial Aerodynamics, 158, pp.11-25.
10) Wang, W., Xue, Y., He, C. and Zhao, Y. (2022). Review of the Typical Damage and Damage-Detection Methods of Large Wind Turbine Blades. Energies, 15(15), p.5672.